TECHNISCHE UNIVERSITÄT DRESDEN

DRESDEN concept
SCIENCE AND INNOVATION CAMPUS

Christian Düreth[1], Andreas Hornig[1,2] and Maik Gude[1]

[1] TU Dresden - Institute of Lightweight Engineering and Polymer Technology
[2] Center for Scalable Data Analytics and Artificial Intelligence Dresden/Leipzig (ScaDS.AI)

Gaussian Process Regression for Multi-Modal Fatigue Crack Growth Identification in Textile-Reinforced Composites

1st of September | Bristol - AIComp 2025

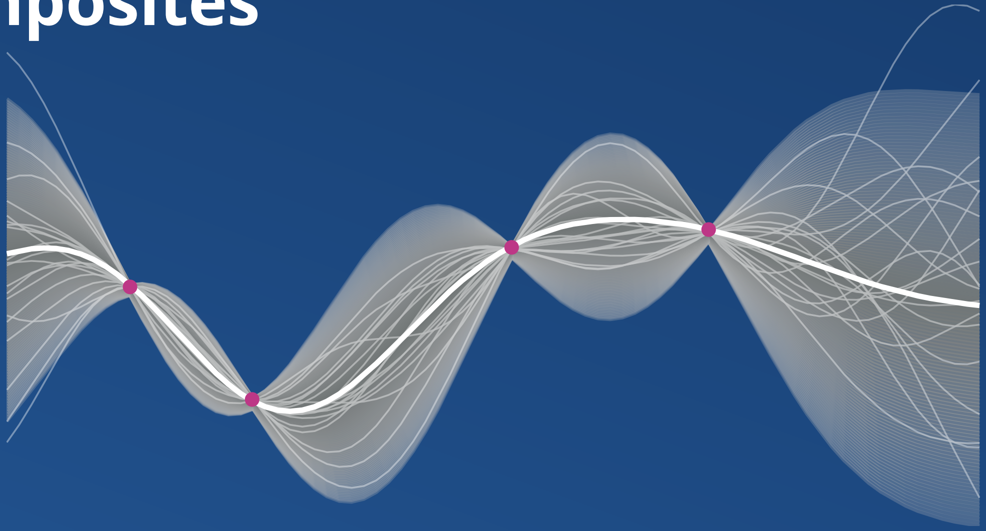

Introduction

- **Context**
  - Textile-reinforced composites: lightweight, high-performance, used in aerospace & wind energy
  - Fatigue crack growth governs lifetime and structural integrity - mainly delamination
- **Challenge**
  - Crack growth is non-uniform [5, 2, 4, 6]
  - Small increments interrupted by **crack jumps**
  - Regimes of slow growth alternating with accelerated propagation
  - Patterns are partly periodic but also irregular, due to textile architecture
  - Multi-modal fatigue data e.g. load–displacement, DIC is noisy and scarce
  - Difficult to detect and model small-scale crack growth regimes with classical window-sized kernels or parametric regression-type models

Machine Learning based data-driven approach like **Gaussian Process Regression with different sparse or uncertain data**

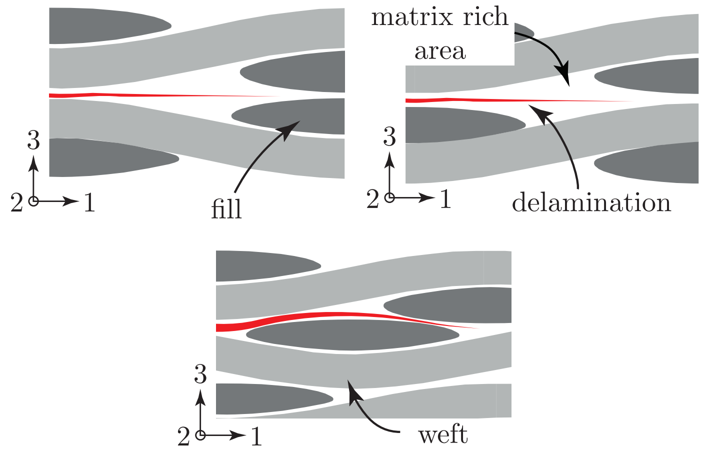

Figure: Idealized textile layer configurations of plain weave textiles

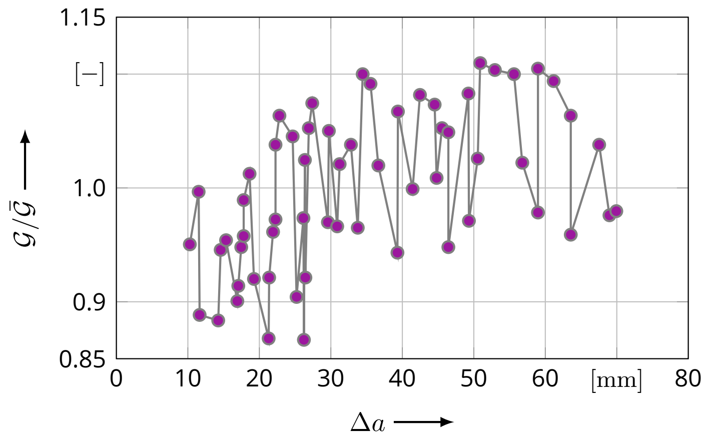

Figure: Exemplary R-curve from quasi-static DCB-test normalized to mean ERR $\bar{\mathcal{G}}$

Material | Selection & Manufacturing

- Areal weight: higher values lead to increased undulation and reduced nesting (and vice versa) [2, 1]
- Manufacturing: resin transfer molding (RTM-6, Hexcel®) in a closed tool of $(530 \times 530 \times 4)\,\mathrm{mm}^3$
- Pre-crack insert: Teflon® foil for DCB specimens
- Adhesive: load blocks bonded with 3M DP490

Table: Material selection for investigating the influence of the fabric architecture on the delamination propagation

Type	Color	ECC-Style†	Areal Density	Spacing	Yarn	Idealized Yarn Geometry‡
I		447	$160\,\frac{\mathrm{g}}{\mathrm{m}^2}$	4 threads/cm		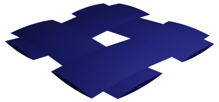
II		450	$200\,\frac{\mathrm{g}}{\mathrm{m}^2}$	5 threads/cm	Pyrofil® TR30S	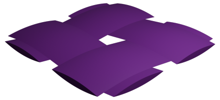
III		460-5	$245\,\frac{\mathrm{g}}{\mathrm{m}^2}$	6 threads/cm		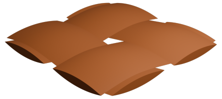

†: Engineered Cramer Composites
‡: images are normalized to column width, do not represent actual geometry of fabrics; created with TexGen and Blender

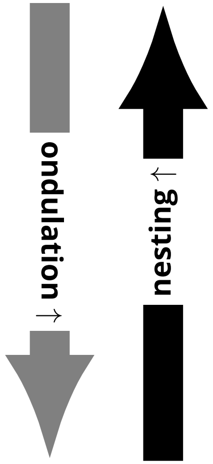

Fatigue Experiments | Set-Up

- **Double Cantilever Beam (DCB) Test**: according to ASTM D5528
- **Testing Machine**: PSB100 (Schenck)
  - Load cell: 100 kN
  - Maximum load amplitude: 50 mm at 10 Hz
  - Force transducer: 2 kN
- **Optical Measurement System**
  - Camera: Nikon DSLR D7000 with (6000 × 4000) Px^2
  - Lens: AF-S Micro NIKKOR 60 mm
  - Camera control: gPhoto2 on Nvidia Jetson Nano (USB-Interface)
  - Triggering: GPIO with digital input from testing machine
  - Post-Processing with RCNN and ZEISS Correlate
- **Fatigue Experiment Control**
  - Pre-cracking step: displacement-controlled (δ_y)
  - Image acquisition before each load block ($n = 1000$ cycles)
  - Load block: force-controlled (P_y) with $R = 0.1$ at 1 Hz
  - Up to $k = 500$ load blocks

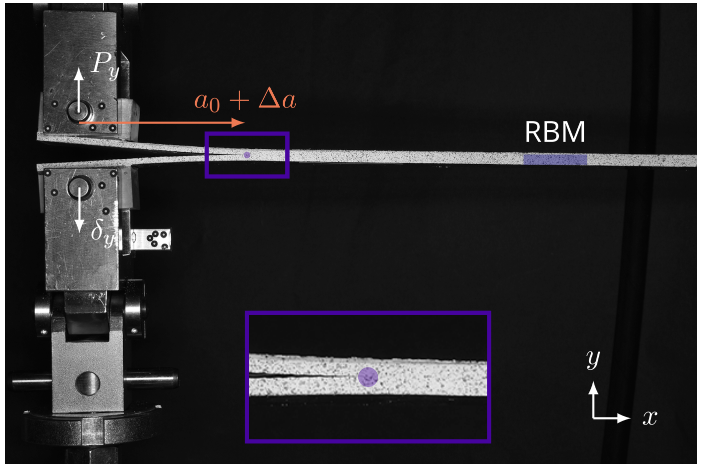

Figure: Experimental set-up and notation

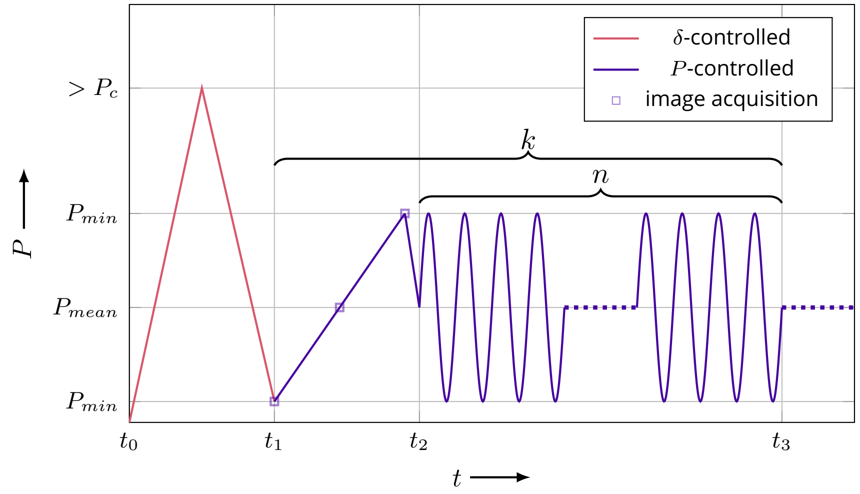

Figure: Fatigue experiment control and monitoring.

Fatigue Experiments | Evaluation of $\mathcal{G}$ via MCC

- **Modified Compliance Calibration (MCC)** from quasi-static tests with optical crack length observations
- **Linear regression** on the calibration dataset $\mathcal{D}^{(c)} = \{(\mathbb{C}_i, a_i)\}_{i=1}^{m}$ for each material $c \in \{\text{I}, \text{II}, \text{III}\}$:

$$\frac{a}{h} = \zeta \sqrt[3]{\mathbb{C}} + \kappa$$

- **Uncertainty estimation** via standard error of the modified CC regression fit

	Type I	Type II	Type III
ζ	29.902	28.143	27.907
σ	0.528	0.310	0.511

- **Compliance in fatigue experiments** obtained from hysteresis curve (unloading branch)
- **Calculation of** G via MCC:

$$\mathcal{G}_{\text{min/max}} = \frac{3\, P^2_{\text{min/max}} \sqrt[3]{\mathbb{C}^2}}{2\, \zeta\, wh}$$

- **Energy release rate range**:

$$\Delta\mathcal{G} = \mathcal{G}_{\text{max}} - \mathcal{G}_{\text{min}},$$

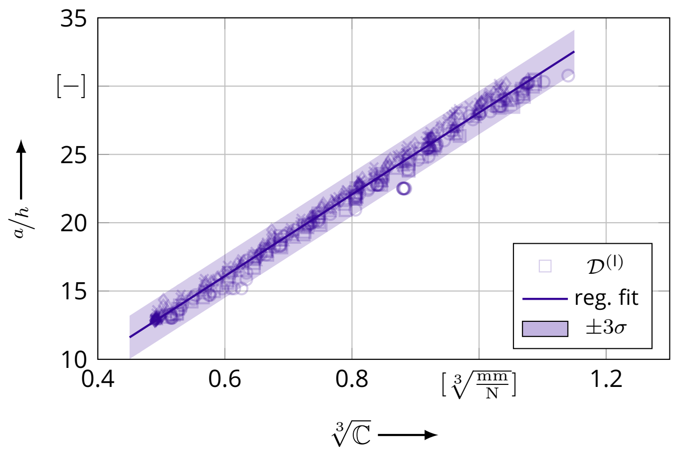

Figure: Results of CC for a $\mathcal{D}^{(1)} = \{(N_i, a_i)\}_{i=1}^{m_k}$.

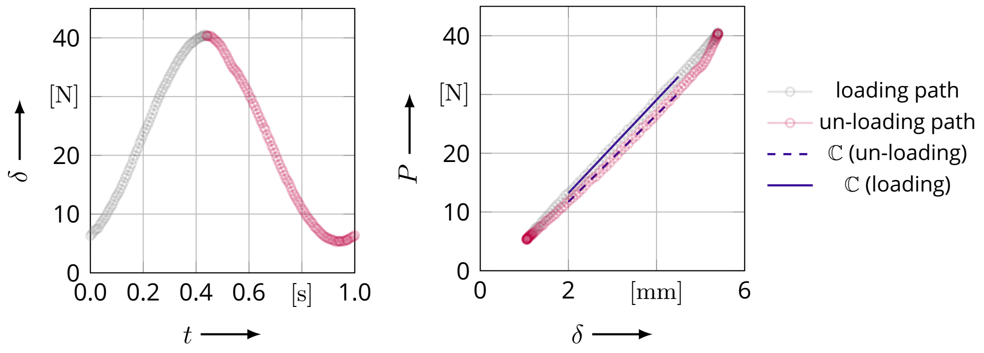

Figure: Exemplary compliance extraction from fatigue hysteresis curve ($N = 300$)

Fatigue Experiments | Evaluation of a via optical methods

- Crack tip detection using a tailored recurrent convolutional network with a YOLO-like head (to be published)
- Optical crack tip measurements discretized every 1000 load cycles
- Post-processing in Zeiss Correlate with rigid body motion tools
- **Estimating the uncertainty:** The standard error of the optical crack tip detection is derived from the mean validation L^1 loss of $\approx$ 0.1 Px, corresponding to a spatial deviation of $\approx$ 0.2 mm.

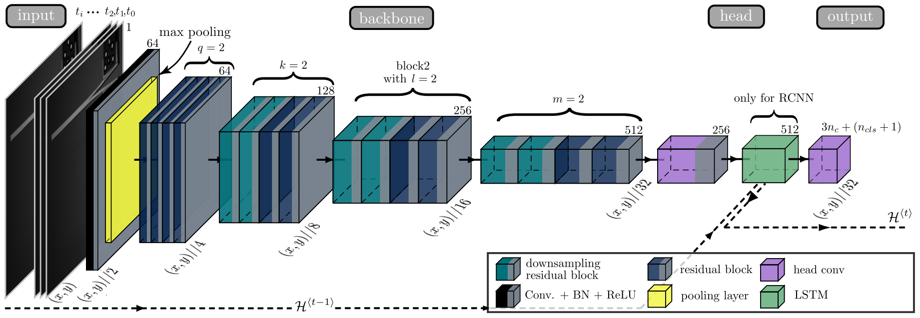

Figure: Schematic Illustration of RCNN

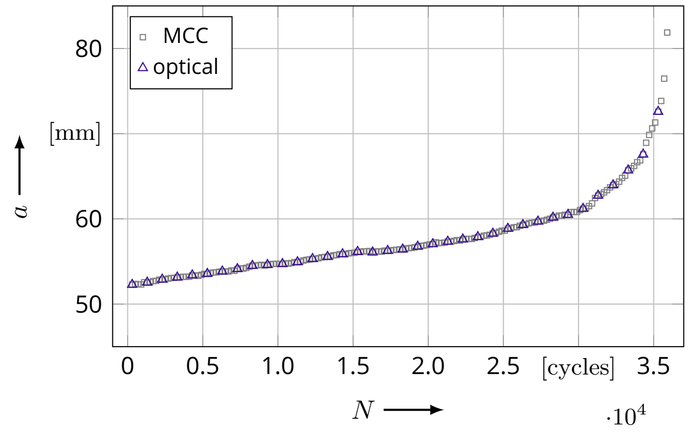

Figure: Exemplary results of the obtained $a - N$-curve for type I

Gaussian Process Regression

- Advantages over kernel-size heuristics or parametric regression:
  - No need to predefine window size or filtering parameters
  - Non-parametric $\Rightarrow$ adapts complexity to data
  - Provides predictive uncertainty (confidence intervals)
  - Applicable also for sparse data
- Gaussian Process Regression with $\mathcal{D} = \{(N_i, a_i)\}_{i=1}^m = \{(\mathbf{x}, \mathbf{y})\}_{i=1}^m$

$$f(\mathbf{x}) \sim \mathcal{GP}(m(\mathbf{x}), k(\mathbf{x}, \mathbf{x}'))$$

- Training by minimizing the **negative log marginal likelihood (NLML)**:

$$\mathcal{L}(\theta) = -\log p(\mathbf{y} \mid \mathbf{X}, \theta)$$

- **Preprocessing:** standardize to $\mathcal{N}(0,1)$ for stability

$$\tilde{\mathbf{x}} = \frac{\mathbf{x} - \mu}{\sigma}, \quad \tilde{\mathbf{y}} = \frac{\mathbf{y} - \mu}{\sigma}$$

- Implementation in **GPyTorch** [3] for PyTorch-based GPU-acceleration

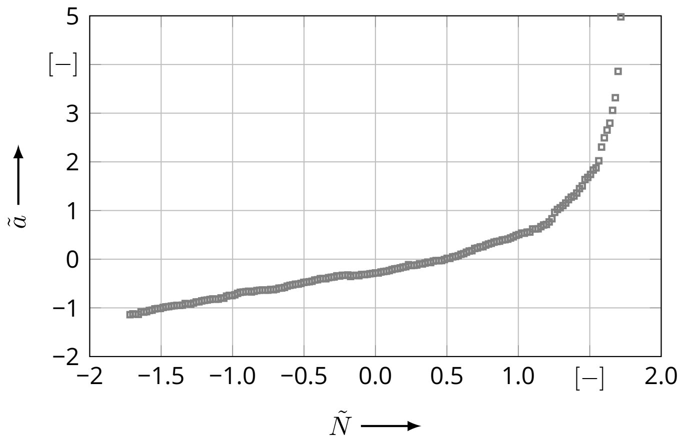

Figure: Normalized dataset $\mathcal{D} = \{(\tilde{N}_i, \tilde{a}_i)\}_{i=1}^m = \{(\tilde{\mathbf{x}}, \tilde{\mathbf{y}})\}_{i=1}^m \sim \mathcal{N}(0,1)$

- **Physics-informed prior** (mean function: $m(\mathbf{x})$): encode expected exponential growth in the GP mean and let the kernel model residuals
- **Kernel function** $k(\mathbf{x}, \mathbf{x}')$ must still be carefully chosen, as it encodes prior assumptions about smoothness and correlation.

Gaussian Process Regression | Kernel & Mean Function Selection

- **Physics-informed mean (prior):**

$$m(\mathbf{x}) = \alpha \, \exp(\beta \, x)$$

- **Kernel functions:**
  - **RBF (squared exponential)**

$$k_{\mathrm{RBF}}(\mathbf{x}, \mathbf{x}') = \sigma_f^2 \exp\left(-\frac{\|\mathbf{x} - \mathbf{x}'\|^2}{2\ell^2}\right)$$

  - **Periodic (sinusoidal)**

$$k_{\mathrm{Per}}(\mathbf{x}, \mathbf{x}') = \sigma_f^2 \exp\left(-\frac{2}{\ell^2} \sin^2\left(\frac{\pi}{p} \|\mathbf{x} - \mathbf{x}'\|\right)\right)$$

  - **Combined kernel (as used):**

$$k(\mathbf{x}, \mathbf{x}') = k_{\mathrm{RBF}}^{(1)}(\mathbf{x}, \mathbf{x}') \; + \; k_{\mathrm{RBF}}^{(2)}(\mathbf{x}, \mathbf{x}') \, k_{\mathrm{Per}}(\mathbf{x}, \mathbf{x}')$$

- **Training (GP):**
  - Optimizer: Adam with learning rate $lr = 1 \times 10^{-2}$
  - Maximum number of iterations: 1000
  - Early stopping when improvement in marginal log-likelihood satisfies

$$|\mathcal{L}_{i-1} - \mathcal{L}_i| < 10^{-4}$$

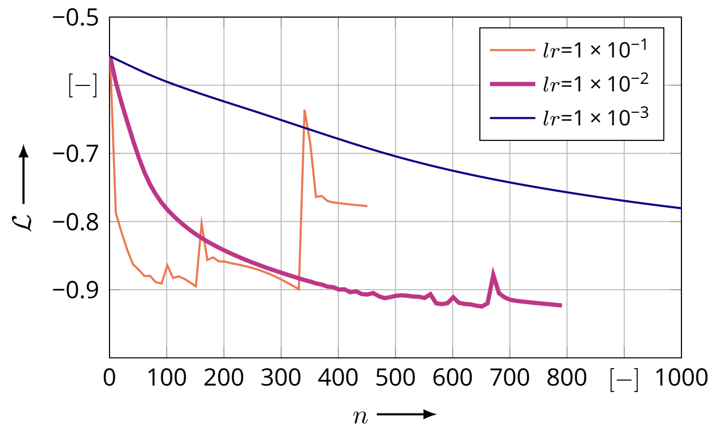

Figure: Training results of $\mathcal{GP}(m(\mathbf{x}), k(\mathbf{x}, \mathbf{x}'))$

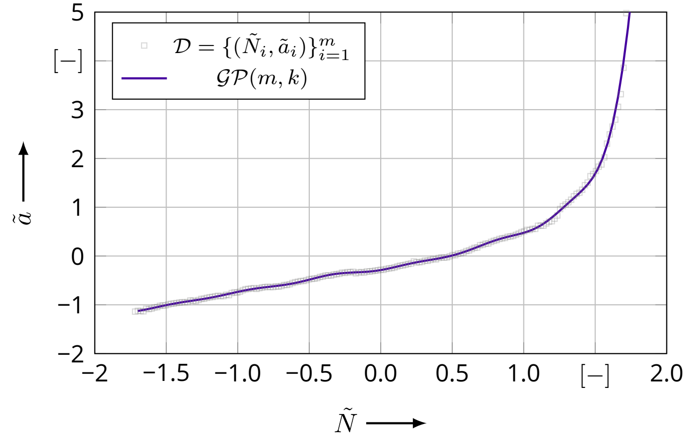

Figure: Inference results of $\mathcal{GP}(m(\mathbf{x}), k(\mathbf{x}, \mathbf{x}'))$

Results |type I

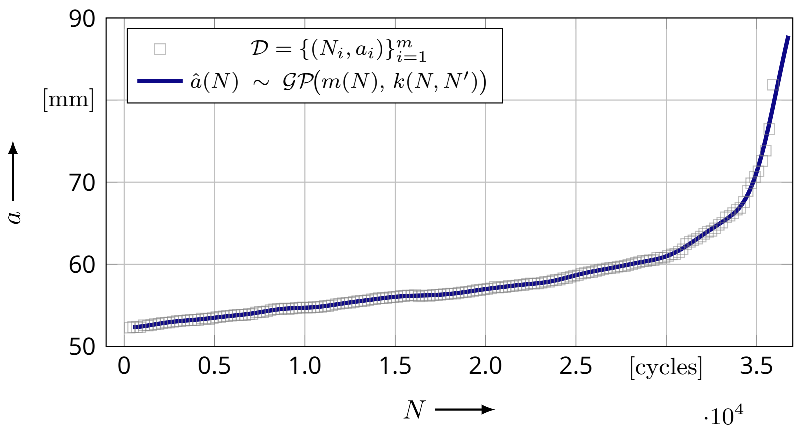

Figure: $a - N$-curve for type I

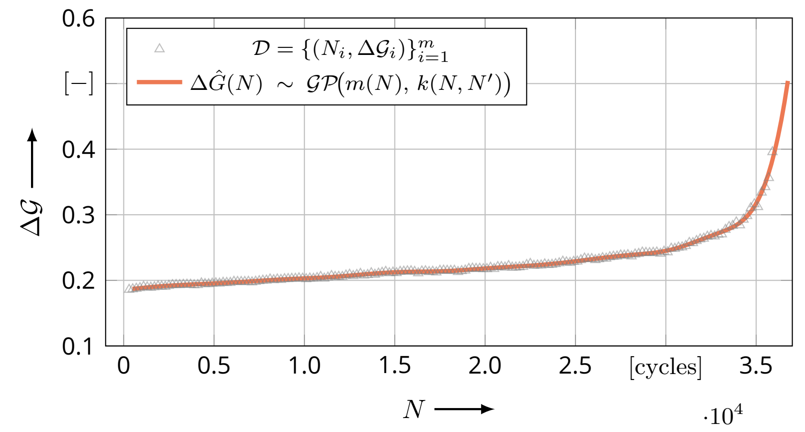

Figure: $N - \Delta G$-curve for type I

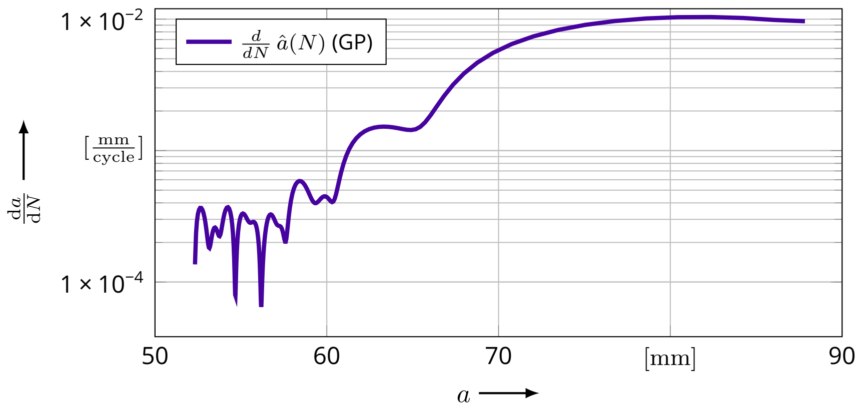

Figure: $a - \frac{da}{dN}$-curve for type I

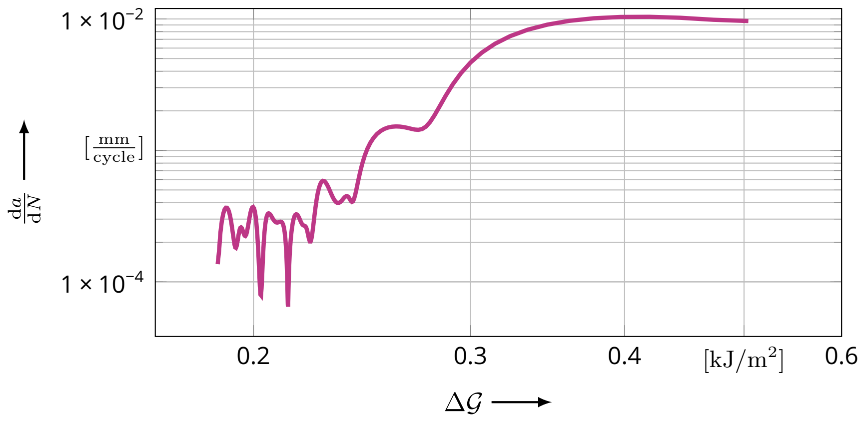

Figure: $\Delta G - \frac{da}{dN}$-curve for type I

Results

- Comparative analysis of material types I–III under identical load amplitude ($P_{\max} \sim 0.8\,\mathcal{G}_c$)
- Observed trend in crack-growth behaviour: lower $\frac{\mathrm{d}a}{\mathrm{d}N}$ with decreasing ondulation length, indicating a retardation effect of textile waviness
- Clear distinction of crack-growth regimes (**crack jumps**) visible in the $\Delta\mathcal{G}$–$\frac{\mathrm{d}a}{\mathrm{d}N}$ relationship
- Data-driven GPR modelling highlights sensitivity of fatigue life to reinforcement architecture
- Small oscillations during the first ~ 1000 cycles indicate running-in effects $\Rightarrow$ assignment of higher uncertainty in this region
- Additional data required for a more robust statistical analysis, in particular for higher cycle counts or loads

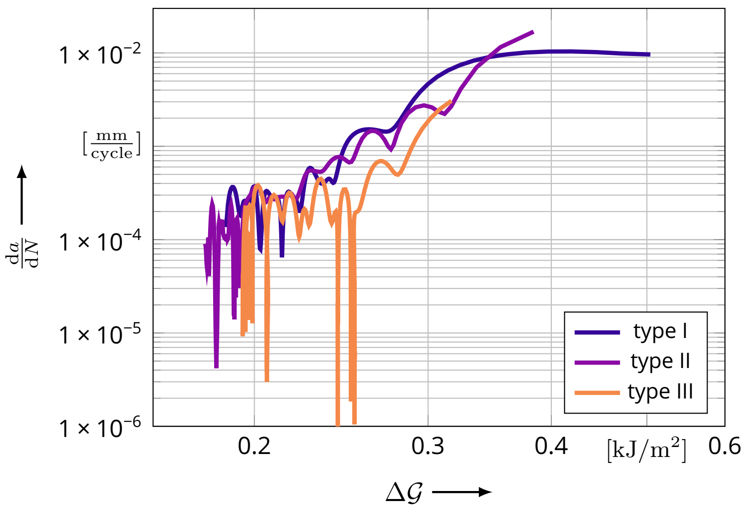

Figure: $\Delta G - \frac{\mathrm{d}a}{\mathrm{d}N}$-curve for type I-III

Conclusion

- Developed a **data-driven framework** using Gaussian Process Regression (GPR) with **physics-informed mean functions** as priors for crack propagation in DCB tests on plain-weave composites
- Fused multimodal data: mechanical compliance curves (higher uncertainty) and optical crack-tip measurements (sparser but more precise)
- Kernel design (RBF, sinusoidal) with exponential mean function (physics-informed prior) shown sufficient to represent the characteristic crack-growth behaviour
- Enabled both predictive interpolation and physics-consistent extrapolation of fatigue crack growth
- Comparative analysis across three plain-weave textile composites with varying areal weight

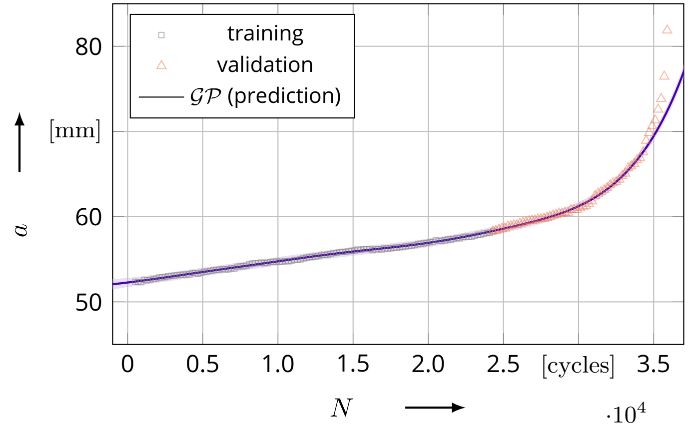

Figure: Extrapolation inference of $\mathcal{GP}\left(m(\mathbf{x}), k(\mathbf{x}, \mathbf{x}')\right)$

- **Outlook**:
  - Analysis of a higher number of tests for data-driven differentiation of textile material behaviour
  - extension to ENF and further advanced fatigue experiments [6]

The group of M. Gude thank the German Research Foundation DFG, which supported this work under Grants GU 614/30-1 (DFG project number: 450147819)

References

[1] Düreth, C., Condé-Wolter, J., Danczak, M., Tittmann, K., Jaschinski, J., Hornig, A., Gude, M., 2025. Analysis of the Compaction Behavior of Textile Reinforcements in Low-Resolution In-Situ CT Scans via Machine-Learning and Descriptor-Based Methods. URL: http://arxiv.org/abs/2508.10943, doi:10.48550/arXiv.2508.10943. arXiv:2508.10943 [cs].

[2] Düreth, C., Weck, D., Böhm, R., Thieme, M., Gude, M., Henkel, S., Wolf, C.H., Biermann, H., 2020. Determining the Damage and Failure Behaviour of Textile Reinforced Composites under Combined In-Plane and Out-of-Plane Loading. Materials 13, 4772. doi:https://doi.org/10.3390/ma13214772.

[3] Gardner, J.R., Pleiss, G., Bindel, D., Weinberger, K.Q., Wilson, A.G., 2021. GPyTorch: Blackbox Matrix-Matrix Gaussian Process Inference with GPU Acceleration. URL: http://arxiv.org/abs/1809.11165, doi:10.48550/arXiv.1809.11165. arXiv:1809.11165 [cs].

[4] Olave, M., Vara, I., Husabiaga, H., Aretxabaleta, L., Lomov, S.V., Vandepitte, D., 2015a. Nesting effect on the mode I fracture toughness of woven laminates. Composites Part A: Applied Science and Manufacturing 74, 166–173. URL: http://linkinghub.elsevier.com/retrieve/pii/S1359835X15001062, doi:10.1016/j.compositesa.2015.03.017.

[5] Olave, M., Vara, I., Usabiaga, H., Aretxabaleta, L., Lomov, S.V., Vandepitte, D., 2015b. Mode I fatigue fracture toughness of woven laminates: Nesting effect. Composite Structures 133, 226–234. URL: https://linkinghub.elsevier.com/retrieve/pii/S0263822315006194, doi:10.1016/j.compstruct.2015.07.073.

[6] Wolf, C.H., Düreth, C., Wünsche, M., Henkel, S., Tittmann, K., Gude, M., Biermann, H., 2025. Fatigue delamination growth in textile-reinforced plastics under combined interlaminar shear and compression: Numerical and experimental characterization. Composite Structures 371, 119384. URL: https://linkinghub.elsevier.com/retrieve/pii/S0263822325005495, doi:10.1016/j.compstruct.2025.119384.

Thank you for your attention!